AFRL-RY-WP-TP-2013-0158

METAMATERIALS, SPATIAL DISPERSION, AND NEGATIVE REFRACTION (PREPRINT)

John Derov

Electro-Optic Components Branch
Aerospace Components & Subsystems Division

Teresa O'Donnell

Air Force Life Cycle Materials Command
Hanscom, AFB

Beverly Turchinetz

Analog Devices

AUGUST 2013
Interim

AIR FORCE RESEARCH LABORATORY
SENSORS DIRECTORATE
WRIGHT-PATTERSON AIR FORCE BASE, OH 45433-7320
AIR FORCE MATERIEL COMMAND
UNITED STATES AIR FORCE

REPORT DOCUMENTATION PAGE

Form Approved
OMB No. 0704-0188

1. REPORT DATE *(DD-MM-YY)*	2. REPORT TYPE	3. DATES COVERED *(From - To)*
August 2013	Technical Paper Preprint	1 October 2011 – 1 June 2013

4. TITLE AND SUBTITLE
METAMATERIALS, SPATIAL DISPERSION, AND NEGATIVE REFRACTION (PREPRINT)

5a. CONTRACT NUMBER
In-house

5b. GRANT NUMBER

5c. PROGRAM ELEMENT NUMBER
61102F

6. AUTHOR(S)
John Derov (AFRL/RYDP)
Teresa O'Donnell (Hanscom, AFB)
Beverly Turchinetz (Analog Devices)

5d. PROJECT NUMBER
3001

5e. TASK NUMBER
12

5f. WORK UNIT NUMBER
Y044

7. PERFORMING ORGANIZATION NAME(S) AND ADDRESS(ES)
Electro-Optic Components Branch
Aerospace Components & Subsystems Division
Air Force Research Laboratory, Sensors Directorate
Wright-Patterson Air Force Base, OH 45433-7320
Air Force Materiel Command, United States Air Force

Hanscom AFB
Analog Devices

8. PERFORMING ORGANIZATION REPORT NUMBER
AFRL-RY-WP-TP-2013-0158

9. SPONSORING/MONITORING AGENCY NAME(S) AND ADDRESS(ES)
Air Force Research Laboratory
Sensors Directorate
Wright-Patterson Air Force Base, OH 45433-7320
Air Force Materiel Command
United States Air Force

10. SPONSORING/MONITORING AGENCY ACRONYM(S)
AFRL/RYDP

11. SPONSORING/MONITORING AGENCY REPORT NUMBER(S)
AFRL-RY-WP-TP-2013-0158

12. DISTRIBUTION/AVAILABILITY STATEMENT
Approved for public release; distribution unlimited.

13. SUPPLEMENTARY NOTES
PAO Case Number 88ABW-2013-3465, Clearance Date 6 August 2013. Report contains color.

14. ABSTRACT
Spatial dispersion, anisotropy, and negative refraction with negative group velocity have been observed in metamaterials. Spatial dispersion occurs when permittivity $\varepsilon(\omega, k)$ and permeability $\mu(\omega, k)$ are dependent on frequency, ω, and wave vector, k, related to a fixed periodic potential along a lattice. The potential along the lattice results from an exciton, resonance, or atomic polarization forming an electric dipole moment. The dipole moments produce a spatially dispersive longitudinal and transverse wave allowing an incident, longitudinal and transverse to exist in the metamaterial. The resonance of Split-Ring-Resonators (SRRs) in SRR-Wire-Post (WP) medium provides the dipole moment needed for spatial dispersion and $\mu < 0$ for negative refraction. The WP is designed to have $\varepsilon < 0$ at the resonant frequency of the SRR providing simultaneous $\varepsilon < 0$ and $\mu < 0$ for negative refraction. We ran parametric simulations changing the geometric parameters of the SRR and WP and used the simulated results to demonstrate the coexistence of spatial dispersion and negative refraction in a SRR-WP medium. The results show the interaction of spatial dispersion and negative refraction in SRR-WP media. We show this by controlling the geometrical parameters of the SRR and WP conditions can be met to differentiate the behavior between spatial dispersion and negative refraction in the SRR-WP media.

15. SUBJECT TERMS
metamaterials, spatial dispersion, negative refraction, split-ring-resonators

16. SECURITY CLASSIFICATION OF:			17. LIMITATION OF ABSTRACT:	18. NUMBER OF PAGES	19a. NAME OF RESPONSIBLE PERSON (Monitor)
a. REPORT	b. ABSTRACT	c. THIS PAGE			John Derov
Unclassified	Unclassified	Unclassified	SAR	18	19b. TELEPHONE NUMBER *(Include Area Code)* N/A

Metamaterials, Spatial Dispersion and Negative Refraction

John S. Derov*

Air Force Research Laboratory, Sensors Directorate, Wright Patterson AFB, OH 45433

Teresa H. O'Donnell*

Air Force Life Cycle Materiels Command, Hanscom AFB, MA 01731

Beverly W. Turchinetz*

Analog Devices, 804 Woburn St., Wilmington, MA 01887

(Dated: July 25, 2013)

Abstract

Spatial dispersion, anisotropy, and negative refraction with negative group velocity have been observed in metamaterials. Spatial dispersion occurs when permittivity $\epsilon(\omega, k)$ and permeability $\mu(\omega, k)$ are dependent on frequency, ω, and wave vector, k, related to a fixed periodic potential along a lattice. The potential along the lattice results from an exciton, resonance, or atomic polarization forming an electric dipole moment. The dipole moments produce a spatially dispersive longitudinal and transverse wave allowing an incident, longitudinal and transverse to exist in the metamaterial. The resonance of Split-Ring-Resonators (SRRs) in SRR-Wire-Post (WP) medium provides the dipole moment needed for spatial dispersion and $\mu < 0$ for negative refraction. The WP is designed to have $\epsilon < 0$ at the resonant frequency of the SRR providing simultaneous $\epsilon < 0$ and $\mu < 0$ for negative refraction. We ran parametric simulations changing the geometric parameters of the SRR and WP and used the simulated results to demonstrate the coexistence of spatial dispersion and negative refraction in a SRR-WP medium. The results show the interaction of spatial dispersion and negative refraction in SRR-WP media. We show this by controlling the geometrical parameters of the SRR and WP conditions can be met to differentiate the behavior between spatial dispersion and negative refraction in the SRR-WP media.

PACS numbers: 78.61.Pt

I. INTRODUCTION

In Veselago's seminal paper[1] on Left-Handed material, he described a material with simultaneously negative permeability (μ) and permittivity (ϵ) in a left-handed coordinate system. The Left-Handed material described by Veselago with a negative refractive index has two required conditions, ϵ and μ must be simultaneously negative and it must have a negative group velocity. Veselago also indicated, aside from a negative refractive material, materials exhibiting anisotropy and spatial dispersion have a negative group velocity as well. In 2000, the first left-handed material, or metamaterial, with simultaneous negative ϵ and μ, was demonstrated using Split-Ring-Resonators (SRRs) and Wire-Post(WP)[2–4]. At resonance, the SRRs provides negative μ[5] and the WP provides negative ϵ[6] producing negative refraction in a metamaterial, which has been demonstrated in the literature[3]. Veselago's model only accounted for the frequency dependence of $\epsilon(\omega)$ and $\mu(\omega)$ in a metamaterial. To describe the behavior observed for ϵ and μ, a bi-anisotropic model[7,8] and spatial dispersion[9–12] models were used. Spatial dispersion has provided the best explanation for the behavior of ϵ and μ in a SRR-WP metamaterial. Alù's model[11,12] used both ϵ and μ to determine frequency and spatially dependent behavior of a metamaterial. Since spatial dispersion and negative refraction are dependent on the resonance of the SRRs and negative group velocity in the metamaterial, SRR-WP media were chosen to study the interaction between the spatial dispersion and negative refractive index in metamaterials. Periodic SRR-WP media were used to determine how, or if, spatial dispersion can be differentiated from negative refraction in a metamaterial. The dispersion in a typical material $\epsilon(\omega)$ and $\mu(\omega)$ is dependent on frequency ω.

A spatially dispersive material occurs when $\epsilon(\omega, \mathrm{k})$ and $\mu(\omega, \mathrm{k})$ are dependent on frequency ω and a wave vector k, where k is related to a fixed periodic potential along a lattice. The periodic potential in a medium can be produced by an exciton, resonance, or a polarized lattice at the molecular level. The exciton, resonance, or polarized lattice form electric dipole moments at the lattice sites of a medium. In our metamaterial, the SRR resonance provides the fixed potential with period a of the SRR-WP unit cell, which determines k, where $k = 2\pi/a$ meeting the condition for spatial dispersion in the medium. Since the conditions for spatial dispersion and negative refraction are related to ϵ and μ, we used ϵ and μ to study the spatial dispersion and negative refraction in metamaterials.

A diagram of the balanced SRRs with a WP used for this study is shown in Figure 1. As seen in Figure 1a, the balanced SRRs consist of 2 identical rings parallel to each other with their gaps opposing each other. Opposing currents are produced in the rings, creating symmetric field distributions around the SRRs. The WP is placed between the 2 SRRs for symmetry as shown. The orientation of the linearly polarized plane wave used to excite the SRR-WP metamaterial is also shown in Figure 1a. The electric field must be parallel to the WP in order to produce a negative ϵ. Figure 1b shows the unit cell with cubic symmetry, which was used for all the simulated structures. The unit consists a dielectric 0.50 mm thick with a relative $\epsilon = 2.2$ to support the SRRs and WP where the SRRs reside on the outer surface and the WP is in the middle of the dielectric. The rest of the unit cell volume consists of air.

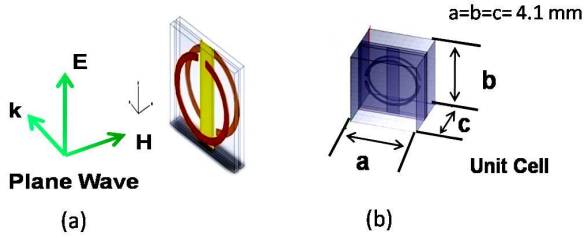

FIG. 1. (a) SRRs with the WP between them and the linear polarized plane wave used to excite the SRRs resonance.(b) SRR-WP unit cell used for the simulations.

In earlier work[13], we fabricated SRR-WP media and measured their transmittance. Snell's law was used to determine the refractive index for the SRR-WP medium. The transmittance and refractive index for the measured and simulated SRR-WP medium and unit cell respectively is shown in Figure 2. The unit cell for the medium in Figure 2 was simulated using Ansyst's High Frequency Structure Simulator (HFSS) and periodic boundary conditions. Though the simulated results in Figure 2 are for the unit cell rather than the medium, comparing the trend in the frequency response between the simulated and measured results show enough agreement to use SRR-WP unit cell simulations to demonstrate spatially dispersive and negative refractive behavior in the SRR-WP media.

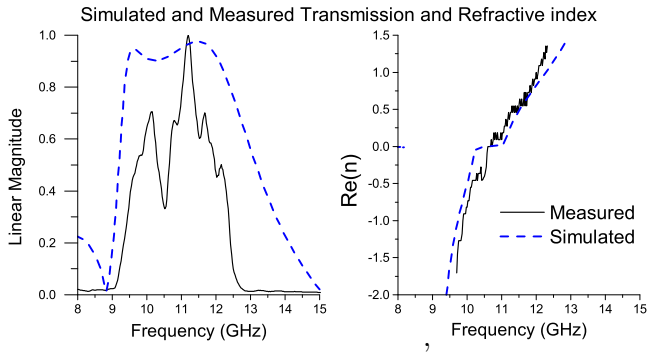

FIG. 2. Measured and Simulated transmission response and real part of the refractive index.

To look at the spatially dispersive behavior and negative refractive index of the SRR-WP structure, parametric simulations were run with varying geometric dimensions of the SRR and WP, holding the dimension of the unit cell constant. The dimensional changes of the SRRs and WP used for the simulation are in Table I.

TABLE I. Dimensions for SRRs, WPs, and Unit Cell

Dimension	OD mm	ID mm	Gap mm	Unit Cell
SRR Size	2.79	2.54	0.51	4.06 mm
	Width mm	Length		
WP Size	0.75	$\approx \infty$		
	0.25 , 0.23, ...0.025	$\approx \infty$		
SRR Size	3.81	3.56	0.51	4.06
WP Size	0.75	$\approx \infty$		

II. SPATIAL DISPERSION

Scattering parameters for the SRR-WP unit cells were obtained from the HFSS simulations. Using a Nicolson-Ross extraction[14], ϵ and μ were determined from the scattering

parameters of the unit cell. The result of the extraction for a unit cell, with a 2.79 mm Outer Diameter (OD) SRR and 0.75 mm wide WP are shown in Figure 3. The frequency and spatial dependence of $\epsilon(\omega, \mathrm{k})$ and $\mu(\omega, \mathrm{k})$ are observed for the unit cell in Figure 3.

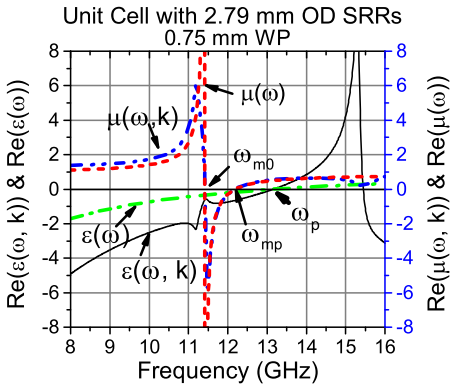

FIG. 3. Spatial and frequency dispersion $\epsilon(\omega,\mathrm{k})$, $\mu(\omega, \mathrm{k})$, $\epsilon(\omega)$, and $\mu(\omega)$ for the unit cell with the 2.79 mm OD SRRs with 0.75 mm WP.

To differentiate the spatial and frequency dependence in $\epsilon(\omega, \mathrm{k})$ and $\mu(\omega, \mathrm{k})$ the frequency dependence of $\epsilon(\omega)$[15] and $\mu(\omega)$[5] were calculated for the unit cell. Equation 1 was used to calculate $\epsilon(\omega)$ for the WP, where ω_p is the plasma frequency for the WP and $\mu(\omega)$ was calculated using equations 2, where ω_{m0} is the resonant frequency of SRRs. To fit $\mu(\omega)$ to $\mu(\omega, \mathrm{k})$, F and γ were varied until $\mu(\omega)$ matched ω_{m0} and ω_{mp} where ω_{mp} is the magnetic plasma frequency.

$$\epsilon(\omega) = 1 - \omega_p^2/\omega^2 \tag{1}$$

$$\mu(\omega) = 1 - F\omega^2/(\omega^2 - \omega_{m0}^2 + \gamma\omega) \tag{2}$$

The spatial dispersion can be observed by comparing the difference in the line shape between $\epsilon(\omega, \mathrm{k})$ and $\epsilon(\omega)$ and $\mu(\omega, \mathrm{k})$ and $\mu(\omega)$ in Figure 3. A resonance is observed in the line shape for $\epsilon(\omega, \mathrm{k})$ that does not occur in $\epsilon(\omega)$ and the resonance in $\epsilon(\omega, \mathrm{k})$ coincides with the resonance in $\mu(\omega, \mathrm{k})$, indicating there is an interaction between the SRRs and WP. The effect of the spatial dispersion on μ can be seen in the deviation of the line shape for $\mu(\omega, \mathrm{k})$ from the Lorentzian line shape of $\mu(\omega)$. To determine why the resonance is occurring in $\epsilon(\omega, \mathrm{k})$ and how it relates to the coupling between the WP and SRRs, a SRR-WP unit cell was simulated without the WP to look at the resonant behavior of the SRRs. The results of

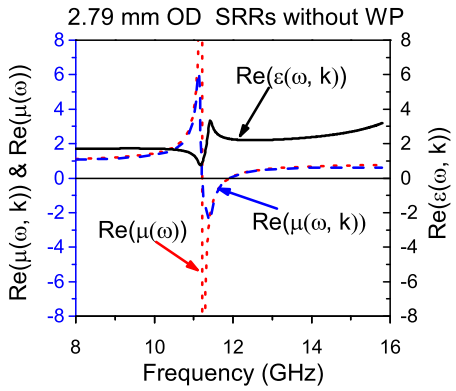

FIG. 4. $\epsilon(\omega, \mathrm{k})$, $\mu(\omega, \mathrm{k})$, and $\mu(\omega)$ for the 2.75 OD SRRs without a WP.

the simulation for the SRRs are shown in Figure 4. Figure 4 shows there is a resonance in ϵ and $\epsilon > 0$, which coincides with the resonance in μ for the SRRs. Indicating the resonance observed in ϵ for the SRR-WP in Figure 3 is associated with the SRRs. Since the resonance for $\epsilon > 0$ in Figure 4 and $\epsilon < 0$ for the resonance observed for the SRR-WP unit cell in Figure 3 requires coupling between the SRRs and the WP for the resonance to occur when $\epsilon(\omega, \mathrm{k}) < 0$. Figure 4 also shows the spatial dispersion is associated with the SRRs since $\mu(\omega, \mathrm{k})$ deviates from the Lorentzian line shape of $\mu(\omega)$ for the SRRs between ω_{m0} and ω_{mp}, which correlates with the frequency range of the resonance in ϵ. The resonance in $\epsilon(\omega, \mathrm{k})$ of the SRR-WP unit cell in Figure 3 shows the WP is coupling with the SRRs, the effect of the coupling between the SRRs and WP was studied by changing the width of the WP.

The width of the WP was varied from 0.75 mm to 0.025 mm for the 2.79 mm OD SRR-WP. Figure 5a and b shows the real part of $\epsilon(\omega, \mathrm{k})$, $\mu(\omega, \mathrm{k})$, $\epsilon(\omega)$, and $\mu(\omega)$ for a 0.25 and 0.13 mm WP width respectively. In Figure 5a the line shape of $\mu(\omega, \mathrm{k})$ is in good agreement with the Lorentzian line shape of $\mu(\omega)$. Comparing the resonance of $\epsilon(\omega, \mathrm{k})$ in Figure 5a and 3, the resonance has decreased and $\epsilon(\omega, \mathrm{k})$ is approaching $\epsilon(\omega)$ below ω_p.

The reduction of the intensity of the resonance for $\epsilon(\omega, \mathrm{k})$ as the WP width was decreased and the agreement of $\mu(\omega, \mathrm{k})$ with $\mu(\omega)$, indicates the spatial dispersion has been reduced to a level where it can be considered negligible. In Figure 5b, the line shape for $\mu(\omega, \mathrm{k})$ does deviate from the Lorentzian line shape of $\mu(\omega)$ and the resonance in $\epsilon(\omega, \mathrm{k})$ shows better

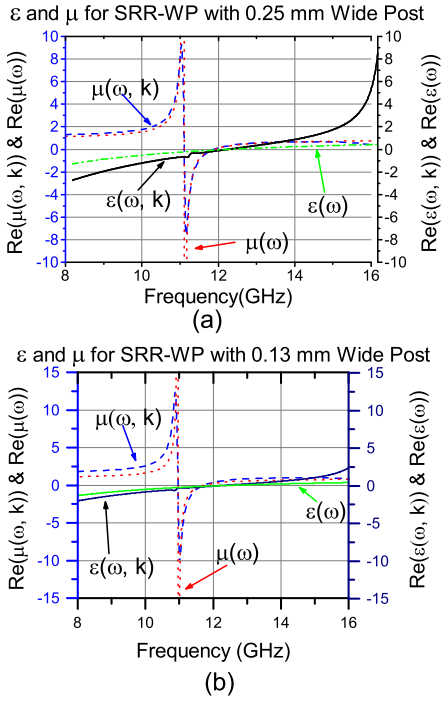

FIG. 5. Real Part of $\epsilon(\omega, \mathrm{k})$, $\mu(\omega, \mathrm{k})$, $\epsilon(\omega)$, and $\mu(\omega)$ for a Unit Cell with 2.79 mm OD SRRs with a) 0.25 mm WP, b) 0.13 mm WP.

agreement with $\epsilon(\omega)$ then $\epsilon(\omega, \mathrm{k})$ in Figure 5a. Though the spatial dispersion is negligible in Figure 5b, value of $\epsilon(\omega, \mathrm{k})$ is approaching 0 between ω_{m0} and ω_{mp} as the width of the WP decreased. As $\epsilon(\omega, \mathrm{k}) \rightarrow 0$ the value of the negative refraction index -n $\rightarrow 0$.

As stated, early spatial dispersion occurs due to the resonance in $\epsilon(\omega, \mathrm{k})$, which creates an electric dipole moment along the WP in the unit cell producing the spatial dispersion in the SRR-WP medium. In the metamaterial there is a longitudinal and a transverse wave associated with the spatial dispersion and an incident wave propagating through the medium. The incident wave propagating through the SRR-WP medium excites the resonance in the SRRs, producing the electric dipole moments along the WP and the longitudinal wave in the medium. The period of the longitudinal wave in the medium is given by a the period of the SRR-WP unit cell and provides the spatial dependence for $\epsilon(\omega, \mathrm{k})$ where $k = 2\pi/a$. The frequency of the longitudinal wave is the same as the resonant frequency of the SRRs even though the period of the longitudinal wave is a. The incident and longitudinal wave propagate through the medium at the same frequency, but at different periods. The period

used for the incident wave is its free space wavelength[9] $\lambda = c_0/f$ where c_0 is the speed of light in vacuum and f is the frequency of the incident wave. As the incident wave propagates through the medium, the phase of the incident wave and the phase of the longitudinal wave interact. This is analogous to the way a plane wave propagates through a crystalline lattice. The core wave functions of atoms along the lattice support the phase of the wave as it propagates through the crystal[16] as shown in Figure 6.

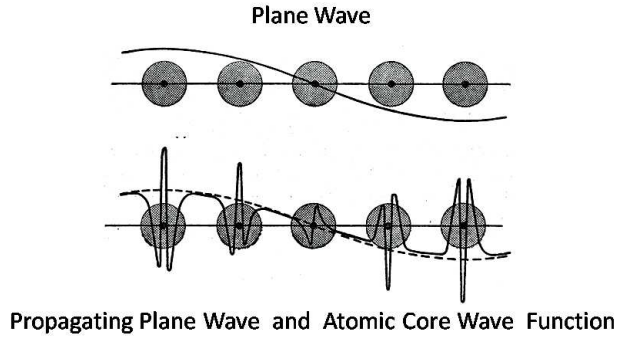

FIG. 6. Plane wave propagation along a crystalline lattice as illustrated by Ziman.

Consider a SRR-WP unit cell in a medium as the atoms in a crystal lattice and the resonance of the SRR-WP are its core wave functions. The interaction between the phase of the incident wave and the longitudinal wave is shown in Figure 7. The period and resonant frequency SRR-WP unit cell in Figure 3 was used to determine the phase response of the medium in Figure 7, making the frequency of the incident wave 11.4 GHz (λ=26.3mm) and the period of the longitudinal wave 4.1 mm. In Figure 7, the maxima and minima for the phase of the incident wave do not lineup with the maxima and minima of the longitudinal wave. The mismatch in the phase of the incident wave with the longitudinal wave shows the incident wave is not totally supported by the longitudinal wave, as the incident wave propagates through the medium, which produces a phase mismatch between the incident and longitudinal wave.

To show the propagation of an incident wave that is supported by the longitudinal wave in the medium, the 4.1 mm period of the unit cell and the condition $a/\lambda < 1$ for spatial dispersion[9] was used to determine the resonant frequency of the SRRs. The resonant frequency determined for the SRRs was 7.2 GHz(λ=41.7mm). In Figure 8, the phase propagation of the 7.2 GHz incident wave and 4.1 mm longitudinal wave for a SRR-WP medium.

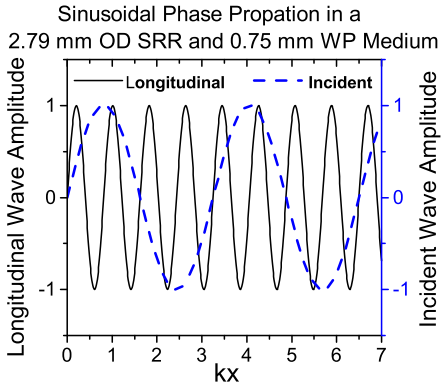

FIG. 7. Phase propagation of the 11.4 GHz incident wave and the 4.1 mm longitudinal wave in a SRR-WP medium.

Figure 8, the maxima and minima of the phase for the incident wave does lineup to the maxima and minima of the phase of the longitudinal. The phase match between the 2 waves indicates that the phase of the incident wave is supported by the longitudinal wave, as it propagates through the medium.

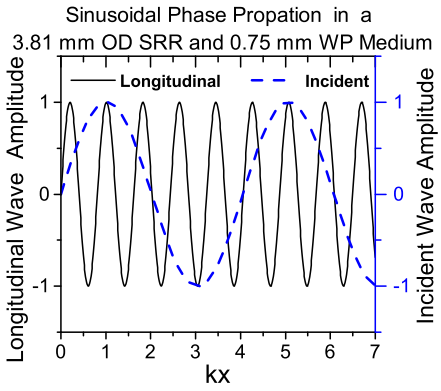

FIG. 8. Phase propagation of the 7.2 GHz incident wave and the 4.1 mm longitudinal wave in a SRR-WP medium.

To match the resonant frequency SRRs to 4.1 mm period of the unit cell, the outer diameter of the SRRs was increased to 3.81 mm. A unit cell for the 3.81 mm OD SRRs with a 0.75 mm wide WP was simulated and $\epsilon(\omega, \mathrm{k})$, $\mu(\omega, \mathrm{k})$, $\epsilon(\omega)$, and $\mu(\omega)$ were determined from the results of the simulation. The real part of $\epsilon(\omega, \mathrm{k})$, $\mu(\omega, \mathrm{k})$, $\epsilon(\omega)$, and $\mu(\omega)$ for the

unit cell is shown in Figure 9. The resonance of $\epsilon(\omega, k)$ is significantly stronger for the 7.2 GHz unit cell then $\epsilon(\omega, k)$ for the 11.4 GHz unit cell in Figure 9.

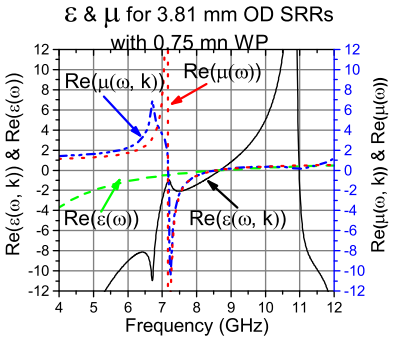

FIG. 9. The real part of $\epsilon(\omega, k)$ and $\mu(\omega, k)$ with the $\epsilon(\omega, k)$ resonance strongly couple to the WP.

III. NEGATIVE REFRACTIVE INDEX

We have discussed spatial dispersion in SRR-WP media and found that the spatial dispersion can be controlled using the geometric dimensions of the SRRs and WP. We also found that negative refraction and spatial dispersion are not independent of each other since the negative refractive index and spatial dispersion occurs within the frequencies of resonance for μ. The negative refractive index occurs for frequencies where $\epsilon(\omega, k)$ and $\mu(\omega, k)$ are simultaneously negative, the refractive index $n=\sqrt{\epsilon\mu}$, n was determined using $\epsilon(\omega, k)$ and $\mu(\omega, k)$when $\epsilon(\omega, k)$ and $\mu(\omega, k)$ simultaneously negative (-)n was assigned to the refractive index. Figure 10 shows the refractive index for the 2.79 mm OD unit cells where the WP width was changed between 0.75 and 0.05 mm. In Figure 3, the frequencies, which refractive index is negative, are between ω_{m0} and ω_{mp} except for the 0.05 mm WP.

Taking a closer look at how the coupling between the SRRs and WP is effected by the change in the WP width, we will look at the frequencies where ϵ and μ are simultaneously negative with respect to the WP width. Using 2.79 mm OD SRR unit cells and their values of ω_{m0}, ω_{mp}, and ω_p, the values of ω_{m0} were plotted as a function of the WP width. Figure 11 shows ω_{m0}, ω_{mp}, and ω_p as a function of the WP width. The frequencies when μ and ϵ are simultaneously negative are shown in Figure 11. In Figure 11, $\mu < 0$ between ω_{m0} and ω_{mp} and for $\omega_p > \omega_{mp}$ $\epsilon < 0$ over all the frequenncies for $\mu < 0$. If $\omega_p < \omega_{mp}$ and $\omega_p > \omega_{m0}$ then $\epsilon < 0$ over only part of the frequency range between ω_{m0} and ω_{mp} as seen in Figure

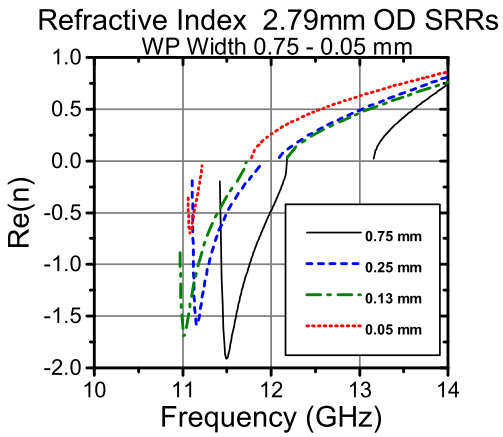

FIG. 10. Refractive Index for the 2.71 mm OD SRRs with WP 0.75, 0.25, 0.13, and 0.05 mm

10 for the 0.05 mm wide WP. Figure 11 also shows the frequency varies for ω_{m0} and ω_{mp} as the WP width changes, but $\Delta\omega_\mu = \omega_{mp}$ - ω_{m0} almost constant and $\Delta\omega_\mu$ is approximately equal to ω_{mp} - ω_{m0} of the SRRs without the WPs. Showing the change in the width of WP causes ω_{m0} and ω_{mp} for the SRRs to shift in frequency relative to ω_{m0} and ω_{mp} for the SRRs without the WP. The interaction between the SRRs and the WP changes when WP = 0.25 mm. For WP widths $>$ 0.25 mm ω_{m0} and ω_{mp} are greater than their values for the SRRs without a WP and for WP widths $<$ 0.25mm ω_{m0} and ω_{mp} are less than their values for the SRRs without the WP.

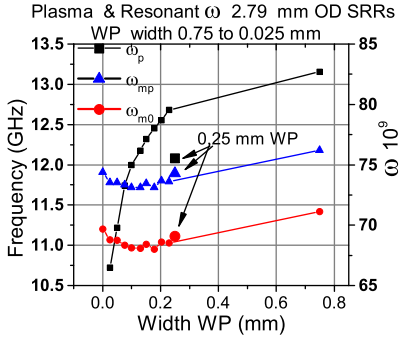

FIG. 11. SRR ω_{mp} and ω_{m0} for the 2.79 mm OD SRRs and WP ω_p for widths from 0.75 to 0.025 mm and the displaced ω_p for the 0.25 mm WP width.

To look at the effect of the SRRs on the WP, ω_p was calculated for the WP widths without the SRRs[6]. Equation 3 was used to determine the ω_p for the WP in the unit cell, where n_{eff} is the effective charge density for WP, e is the electron charge, ϵ_r is the effective

relative permittivity, for the unit cell used in the simulations to account for the dielectric used to support SRRs and WP along with the with the volume of air in the unit cell, ϵ_0 is the permittivity of free space, and m_{eff} is the effective electron mass for the wire.

$$\omega_p^2 = \frac{n_{eff}e^2}{\epsilon_r \epsilon_0 m_{eff}} \tag{3}$$

The n_{eff} is determined by the spatial fraction that the WP occupies in the unit cell and is given in Equation 4 where n is the electron charge density in the WP, L is the width of the wire, W is the thickness of the wire, and a is the period the unit cell.

$$n_{eff} = n\frac{LW}{a^2} \tag{4}$$

The effective m_{eff} is given by equation 5,

$$m_{eff} = \frac{\mu_0 LW e^2 n}{2\pi}\ln(a/r) \tag{5}$$

where μ_0 is the permeability of free space and $r = \sqrt{LW/\pi}$. Substituting equations 4 and 5 into 3, then ω_p is given by equation 6 for WP in the unit cell.

$$\omega_p = \frac{c_0}{a}\sqrt{\frac{2\pi}{\epsilon_r \ln(a/r)}} \tag{6}$$

where c_0 is the speed of light in vacuum. Figure 12 shows the calculated ω_p for the WP without the SRR and ω_p for the simulated SRR-WP as a function of WP width. Looking at the curves in Figure 12 for ω_p, all the plasma frequencies calculated using the WP widths nicely fall on the curve as would be expected.

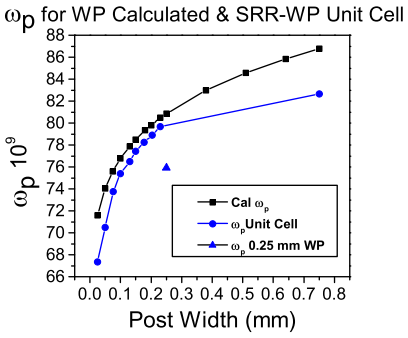

FIG. 12. Plasma frequency vs. post width for SRR-WP unit cell for post widths from 0.75 mm to 0.025 mm and calculated for post wide L=0.75 to 0.025 mm, W= 0.05mm, ϵ_r=1.11.

The curve of the SRRs-WP unit cells shows a response similar to the calculated plasma frequencies for the WP widths form 0.025 to 0.23 mm indicating the WPs are behaving more like their calculated counterparts, until the width of the WP is 0.25 mm. For the WP widths 0.25 and 0.75 mm ω_p shows a stronger interaction with the SRRs. The ω_p of 0.25 and 0.75 mm WP widths for the SRR-WP unit cells show a larger deviation from the calculated ω_p for the WP widths. Both the 0.25 and 0.75 mm WP widths show a strong interaction with the SRRs, but the 0.25 mm WP width shows the strongest interaction with the SRRs. In Figure 11 the 0.25 mm ω_p for the 0.25 mm WP width approaches ω_{mp} for the SRRs where the value of ω_p for the 0.75 mm WP width is closer to its calculated ω_p.

In Figure 4 we showed that the resonance in ϵ was associated with resonance of μ for the SRRs and the SRRs were responsible for the spatial dispersion in the SRR-WP metamaterial. In Figure 5a we showed that the interaction between the 0.25 mm WP virtually removed the spatial dependence in μ by its agreement with $\mu(\omega)$. The disassociation ω_p for the 0.25 mm wide WP, from its calculated behavior in Figure 12 and the result from Figure 5a indicates the behavior of ϵ and μ is localized in the unit cell. Since μ does not have a spatial dependence, it allows ϵ and μ to be treated independently in Maxwell's equations, indicating a medium made from the, 2.79 mm OD and 0.25 mm WP, units cells can be homogeneous. Treating μ as just a frequency dependent parameter provides a way to distinguish the negative refraction in a metamaterial even though ϵ even though ϵ is spatially dependent.

IV. SUMMARY AND CONCLUSION

As discussed, the waves produced by spatial dispersion in the metamaterial have a longitudinal and transverse mode. A plane wave incident on a SRR-WP metamaterial excites the resonance in the SRRs and couples to the WP creating an electric dipole moment, producing a longitudinal wave in the metamaterial. The coupling between SRRs and WP allows energy from the incident wave to be transferred to the longitudinal wave and the 2 waves interact as they propagate through the metamaterial. When the wavelength of the resonant frequency of the SRRs and the period of the unit cell coincide, the phase of the longitudinal and the incident wave will match, increasing the coupling between the SRR and WP producing a stronger electric dipole moment along the WP. The increased strength of the electric dipole

moment in the unit cell shows the excitation of the SRRs by incident wave is transferring its frequency domain energy to the longitudinal spatial domain wave via μ by the resonance in ϵ.

We also showed the association of negative refraction with spatial dispersion in a metamaterial since the both the negative refractive index and the spatial dispersion depend on the resonance of the unit cell. Varying the width of the WP allowed us to control the spatial dispersion in the SRR-WP medium and by matching the resonant frequency of the SRR-WP with the period of the unit cell the spatial dispersion increased in a SRR-WP medium. Though the spatial dispersion can be maximized and minimized in the SRR-WP medium, the negative refraction and spatial dispersion could not explicitly be separated. By varying the width of WP in the unit cell we determined that a 0.25 mm wide WP minimized the spatial behavior of the SRR-WP unit cell with the 2.79 OD mm SRRs. The coupling between SRRs and the 0.25 mm WP in the unit cell, virtually eliminates the spatial dependence in μ making the negative refractive index distinguishable from the spatial dispersion. Concluding the spatial dispersion and negative refraction in a SRR-WP cannot be explicitly separated, but negative refraction can be distinguished from the spatial dispersion.

ACKNOWLEDGMENTS

I would like to thank Dr. Michael Alexander for his insightful discussions on the physical phenomena. I would also like to thank Dr. Harold Weinstock at AFOSR for his support and making this work possible. Kristina Vogel for her editorial support.

---

* Formerly: Air Force Research Laboratory, Sensors Directorate,Hanscom AFB, MA 01731

[1] V. G. Veselago, Soviet Physics USPEKHI **10**, 6 (1968).

[2] D. Smith and N. Kroll, Physical Review Letters **85** (2000).

[3] S. D. Shelby, R. A. and S. Schulz, Science **292** (2001).

[4] D. R. Smith, W. J. Padilla, D. C. Vier, S. C. Nemat-Nasser, and S. Schultz, Physial Review Letters **84**, 4 (2000).

[5] J. B. Pendry, A. J. Holden, D. J. Robbins, and W. J. Stewart, IEEE TRANSACTIONS ON MICROWAVE THEORY AND TECHNIQUES **47**, 10 (1999).

[6] J. B. Pendry, A. J. Holden, W. Stewart, and I. Youngs, Physical Review Letters **76**, 4 (1996).

[7] F. M. R. Marqués and R. Rafi-El-Idrissi, Physical Review B **65**, 6 (2002).

[8] C. R. Simovski, "Bloch material parameters of magneto-dielectric metamaterials and the concept of bloch lattices," (2007).

[9] V. Ginzburg, PHYSICS REPORTS (Review Section of Physics Letters) **194**, 12 (1990).

[10] V. M. Agranovich and V. L. Ginzburg, *Crystal Optics with Spatial Dispersion and Excitons* (1984).

[11] A. Alù, "Spatial and frequency disperson effects in the homogenization of metamaterial arrays," arxiv.org/ftp/arxiv/papers/1012/1012.1351.pdf.

[12] A. Alù, Physical Review B **83** (2011).

[13] J. Derov, B. Turchinetz, J. Dean, E. Crisman, and A. Drehman, "Free space measured loss comparison of single and double ring resonators for negative index media," IEEE Antennas and Propagation Society International Symposium , June 10-15 (2007), dOI:10.1109/APS.2007.4396794.

[14] A. M. Nicolson and G. F. Ross, IEEE Transactions on Imstrumentation and Measurement **IM-19**, 6 (1970).

[15] C. Kittel, *Introduction to Solid State Physics*, 4th ed. (John Wiley and Sons, New York, 1971).

[16] J. M. Ziman, *Principles of The Theory of Solids*, 2nd ed. (Cambridge University Press, 1972).